ELSEVIER

Polymer 43 (2002) 971–976

polymer

www.elsevier.com/locate/polymer

Molecular dynamics simulation of *cis*-1,4-polybutadiene. 1. Comparison with experimental data for static and dynamic properties☆

Okimasa Okada, Hidemine Furuya*

Department of Organic and Polymeric Materials, Tokyo Institute of Technology, 2-12-1 Ookayama, Meguro-ku, Tokyo 152-8552, Japan

Abstract

Molecular dynamics (MD) calculations of *cis*-1,4-polybutadiene in bulk amorphous phase were performed under constant pressure and constant temperature conditions. The static and dynamic properties were evaluated from the results of MD calculations. The obtained density and coefficient of thermal expansion are in good agreement with experimental data. The feature of the calculated static structure factor is similar to the observed one. Molecular motion is examined with mean square displacements and intermediate scattering functions. An onset of a new motion, which corresponds to so-called fast process, was clearly observed in the temperature dependence of the mean square displacement above 100 K. The dynamic structure factors obtained by the Fourier transformation of the intermediate scattering functions are compared with those obtained from quasielastic neutron scattering measurements. The peaks corresponding to the elastic scattering and the low energy excitation at around 2 meV are reproduced in the dynamic structure factors. The excessive intensity observed in the dynamic structure factor, which corresponds to the fast process, is also reproduced above 140 K in our simulation.

Keywords: *cis*-1,4-Polybutadiene; Molecular dynamics; Dynamic structure factor

1. Introduction

Many studies have investigated the dynamics of amorphous materials at the glass transition. Most of them are phenomenological studies to describe the macroscopic thermal and physical properties by experiments. Recently, so-called mode coupling theory, which is based on the microscopic theory, has been developed [1–3]. This theory utilizes an equation for the density autocorrelation function with a nonlinear memory function and predicts the dynamic process involved in the glass transition. Many experiments have also been performed to examine the dynamic process of glass forming materials using neutron scattering, dielectric relaxation techniques and so on. Some inelastic neutron scattering studies [4–9] have shown that a broad peak corresponding to fast motion has been observed on various kinds of amorphous materials at 1.5–4.0 meV below the glass transition temperature (T_g), which is called low-energy excitation. Kanaya et al. [5] have shown that the low-energy excitation in amorphous polymers is described in terms of phonon assisted tunneling motion in an asymmetric double well potential. At around T_g in the energy range below 2 meV a very fast process has been observed by quasielastic neutron scattering (QENS). Since the relaxation time of the fast process is almost independent of both temperature and scattering vector, the origin has been predicted as localized molecular motions. For *cis*-1,4-polybutadiene (PB) the fast process has been detected above so-called Vogel–Fulcher temperature, which is about 50 K below T_g for most of the materials [10–13]. However, the feature of the molecular motion related to the fast process has not been elucidated yet, because it is difficult to trace the molecular motion at the atomic level by experiments.

Molecular dynamics (MD) calculation is one of the most promising methods to figure out the details of the fast molecular motion. Many MD calculations have been performed on bulk amorphous polymers [14–25]. Mattice et al. have utilized molecular simulations to study the physical properties and molecular motion of PB [14–17] using the conformational analyses and the torsional auto-correlation functions. Gee et al. have performed the MD calculations of PB to examine the conformational dynamics [18]. Roe has employed the MD calculations of poly-ethylene (PE) [19] and polystyrene (PS) [25] for the investigation on the molecular motion by analyzing the mean square displacements, the intermediate scattering

☆ This paper was originally submitted to *Computational and Theoretical Polymer Science* and received on 29 March 2001: received in revised form on 2 June 2001: accepted on 15 June 2001. Following the incorporation of *Computational and Theoretical Polymer Science* into *Polymer*, this paper was consequently accepted for publication in *Polymer*.

* Corresponding author. Tel.: +81-3-5734-2806; fax: +81-3-5734-2888.
E-mail address: hfuruya@polymer.titech.ac.jp (H. Furuya).

0032-3861/02/$ - see front matter
PII: S0032-3861(01)00628-0

functions, and the dynamic structure factors. Recently, Smith et al. have investigated chain dynamics of a 1,4-polybutadiene melt by MD simulations and neutron spin echo experiments [26,27].

In this study the MD calculations of PB in the bulk amorphous phase were performed. The validity of the force filed was confirmed at first by comparing the calculated physical properties with experimental and theoretical studies. The molecular motion is investigated using the mean square displacements, the intermediate scattering functions, and the dynamic structure factors to compare with the results of the QENS [12,13] and other MD studies [16,18,19,25].

2. Method of MD simulation

All the MD calculations were performed using an MD simulation package called GEMS/MD (Nano Simulation Associates, Japan). Molecular structure of PB and the atom types used for the force field are shown in Fig. 1, where the first characters of the atom types correspond to the elements. All the bonded potential parameters are listed in Table 1. The bonded potential parameters were optimized using HF/6-31G* level ab initio calculations in this work. After all the parameters were determined temporarily, the torsional potential parameters were re-optimized by trial and error using the MD calculations to reproduce the experimental ratio of the trans conformation reported by Abe and Flory [28]. The details of the procedures for the determination of the parameters used in the force field have been explained elsewhere [29,30]. The parameters for the van der Waals potential and the partial charges are taken from OPLS-AA force field [31]. These parameters have been optimized to reproduce the experimental density and heat of vaporization of amorphous liquids of small molecules [32]. The standard combination rule used in OPLS-AA was employed for the Lennard–Jones interactions.

All atom model of a single PB molecule having 200 monomer units ($H(–CH_2–CH=CH–CH_2)_{200}–H$) was created. The initial amorphous structure was created using the Monte Carlo method that Li et al. have employed in their molecular simulations of PB [14]. The size of the cell was preliminary determined to realize the experimental density of 0.89 g/cm^3 [33]. The van der Waals radii of the atoms were reduced to 30% of the original ones, which enables us to insert the molecule into the MD cell using the three-dimensional periodic boundary conditions. In order to eliminate the initial deficiencies in the created amorphous structure such as energetically unfavorable dihedral angles and atomic contacts, the molecular mechanics calculation was employed to decrease the potential energy of the system. Then the system was dynamically equilibrated using the MD calculations in the ambient condition to prepare the initial structure for the following MD calculations.

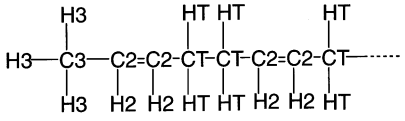

Fig. 1. Definitions of atom types for *cis*-1,4-polybutadiene. The first characters of the atom types represent the elements.

All the MD calculations were performed under constant pressure and constant temperature conditions. The pressure of the MD system was kept at 0.1 MPa. The temperature of the system was set at 300 K for the initial equilibration. The temperature was lowered gradually down to 50 K. The equilibration runs at each temperature were performed for 2 ns before the sampling runs. The duration of the sampling

Table 1
Force field parameters of bonded potential for PB (Atom types are shown in Fig. 1)

Bond stretch[a]	R_0 (Å)	V_B (kcal/mol/Å^2)	
C3–H3	1.080	410	
C3–C2	1.505	362	
C2–H2	1.080	434	
C2–C2	1.320	812	
C2–CT	1.505	356	
CT–HT	1.080	406	
CT–CT	1.540	310	
Angle bending[a]	**θ_0 (deg)**	**V_A (kcal/mol/rad^2)**	
H3–C3–H3	107.5	48.3	
H3–C3–C2	111.3	51.6	
C3–C2–H2	114.4	41.8	
C3–C2–C2	128.5	73.2	
H2–C2–C2	117.1	48.7	
C2–C2–CT	128.5	73.2	
CT–C2–H2	114.4	41.8	
C2–CT–CT	112.1	65.0	
C2–CT–HT	110.1	55.7	
CT–CT–HT	108.9	53.1	
HT–CT–HT	106.4	49.0	
Torsion[a]	**V_1**	**V_2**	**V_3**
CT–C2–C2–CT	0.0	−9.5	0.0
C3–C2–C2–CT	0.0	−9.5	0.0
C3–C2–C2–H2	0.0	−9.5	0.0
H2–C2–C2–CT	0.0	−9.5	0.0
H2–C2–C2–H2	0.0	−9.5	0.0
H3–C3–C2–H2	0.0	0.0	0.318
H3–C3–C2–C2	0.0	0.0	−0.372
C2–C2–CT–CT	0.8063	0.0366	0.876
C2–C2–CT–HT	0.0	0.0	−0.372
H2–C2–C2–H2	0.0	0.0	0.318
H2–C2–CT–CT	0.0	0.0	0.366
C2–CT–CT–C2	1.05	0.511	−0.552
HT–CT–CT–C2	0.0	0.0	0.366
HT–CT–CT–HT	0.0	0.0	0.318
Inversion[a]	**V_I (kcal/mol/rad^2)**		
C2–C2–CT–H2	45.3		

[a] Potential energy functions for bond stretching, bending, torsion, and inversion are defined as $E_B = V_B(R - R_0)^2$, $E_A = V_A(\theta - \theta_0)^2$, $E_T = \sum_{k=1}^{3} V_k \cos(k\phi)$, and $E_I = V_I(\Theta - \Theta_0)^2$, respectively.

runs was 0.5 ns. The methods proposed by Nosé [34,35], Hoover et al. [36] to control temperature and by Andersen [37] to control pressure were employed. For the numerical integration of the Newtonian equation of motion, time steps of 1 and 0.5 fs (1 fs $= 10^{-15}$ s) were chosen for the systems below 235 K and above 260 K, respectively. A cut-off radius for the van der Waals potential of 10 Å was used. The electrostatic interactions were evaluated with the spherical Ewald truncation method [38,39].

3. Results and discussion

3.1. Static physical properties

After 1 ns MD run at 300 K the density of the system became constant indicating that the system was equilibrated. The estimated density at 300 K is 0.90 g/cm^3, which is in excellent agreement with the experimental value of 0.89 g/cm^3 [33]. The temperature of the system was gradually decreased after the system was confirmed to be in the equilibrium state by checking the change of the density at each temperature. The temperature dependence of the density is shown in Fig. 2. The estimated coefficient of thermal expansion at 300 K was 5.2×10^{-4} (K^{-1}). This value is similar to the experimental values of 6.63×10^{-4} (K^{-1}) for *cis*-1,4-polybutadiene [40] and 7.5×10^{-4} (K^{-1}) for a copolymer of *cis*-1,4-, *trans*-1,4-, and vinyl-1,2-polybutadiene [41]. The intersection of the two lines fitted to the plots for the high and low temperature regions at about 195 K corresponds to the glass transition temperature, which is in agreement with the experimental value of 170 K [42] and with the result of the MD simulation of 185 K [43].

The partial radial distribution function (PRDF) $g_{ij}(r)$ shows the probability of finding a pair of atoms in terms of distance:

$$g_{ij}(r) = \frac{V}{N_i N_j} \sum_{j=1}^{N_j} \frac{n_{ij}(r)}{4\pi r^2 \Delta r} \quad (1)$$

where N_i and N_j are the numbers of atoms i and j in cell volume V, $n_{ij}(r)$ is the number of j atoms in the distance between $r - (\Delta r/2)$ and $r + (\Delta r/2)$ from i atoms. The PRDFs for all the pairs of elements of carbon–carbon, hydrogen–hydrogen, and carbon–hydrogen at 300 K are shown in Fig. 3. The PRDFs include the contributions of the intermolecular and intramolecular pairs. The obtained results are basically in good agreement with the results reported by Li et al. [14]. A difference from their results is that one peak in their data for the carbon–carbon atom pair at around 1.4 Å is split into two peaks in our result. In our result, one of the two peaks comes from the bond length for C=C (1.320 Å) and the other from the bond lengths 1.505 and 1.540 Å for C–CH_2 and CH_2–CH_2, respectively. In their data the differences of three bond lengths 1.33, 1.43, and 1.53 Å for C=C, C–CH_2, and CH_2–CH_2, respectively, might be too small to distinguish and be degenerated into one peak. As they have discussed, no correlation for the distribution of atoms is detected in the distance longer than 7 Å in our results.

In order to investigate the structure of the bulk amorphous phase, the neutron diffraction pattern is also calculated by the Fourier transformation of the radial distribution function. The calculated structure factor is shown in Fig. 4, where a sharp peak at about 1.4 Å^{-1} and broad peaks around 3 and 6 Å^{-1} are observed. The peak positions of the calculated pattern are in agreement with the observed data, though the copolymer of *cis*-1,4-, *trans*-1,4-, and vinyl-1,2-polybutadiene was used in the measurement [44].

3.2. Dynamic properties

The mean square displacement (MSD) $\langle \Delta r^2(t) \rangle$ of the

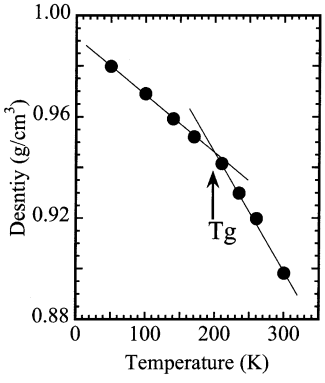

Fig. 2. Temperature dependence of the density obtained from the MD simulation. Intersection indicates glass transition temperature.

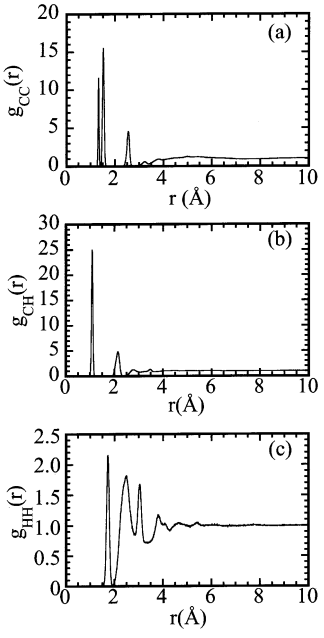

Fig. 3. The partial distribution functions for: (a) carbon–carbon, (b) carbon–hydrogen, and (c) hydrogen–hydrogen atom pairs.

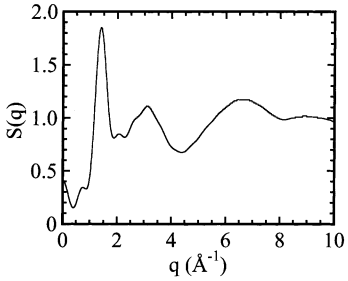

Fig. 4. The structure factor obtained by Fourier transformation of radial distribution function.

atoms is evaluated by:

$$\langle \Delta r^2(t) \rangle = \langle [r_i(t) - r_i(0)]^2 \rangle \quad (2)$$

where $r_i(t)$ is the position vector of the ith atom at time t and the brackets $\langle\ \rangle$ on the right denote the average for all atoms as well as for all time origins. Fig. 5 shows the MSDs of carbon and hydrogen atoms at several temperatures. The temperature dependence of the MSD of hydrogen atoms is almost same as that of carbon atoms except for the magnitude. That is, the MSDs of the hydrogen atoms are larger than those of carbon atoms compared at the same temperature. The trend of the obtained MSDs is similar to the results of the MD calculations of PE [19] and PS [25] reported by Roe. Similar results of MSDs have also been obtained using the QENS studies of polyvinylchloride (PVC) [45,46] and PS [47]. As Roe discussed, two distinct time regimes were also observed in our calculated MSDs. The crossover of the fast and slow regimes lies at around 1 ps. Below 170 K the displacement reversed during the crossover indicating that a recoil motion is taking place. Above 210 K the crossover becomes smooth and the two regimes are not distinguishable. In addition to the recoil

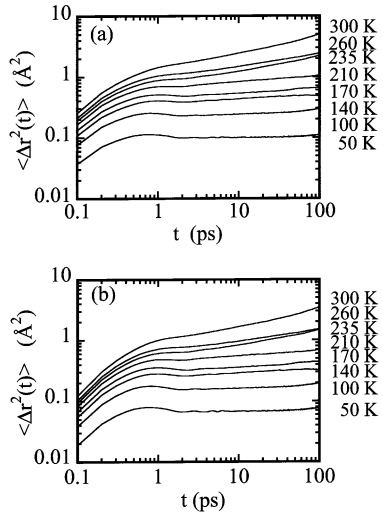

Fig. 5. The mean square displacements for: (a) hydrogen and (b) carbon atoms at several temperatures.

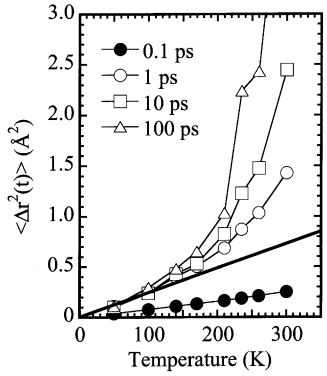

Fig. 6. The mean square displacements as a function of temperature for several fixed values of time.

motion, the conformational changes might be taking place frequently above 210 K.

The slopes of the curves in the fast regime are almost same at all temperatures, while they vary with temperature in the slow regime. At 50 K little displacement is taking place in the slow regime. The positive slopes above 100 K in the slow regime show that the displacement is clearly taking place. This suggests that the α-process is not arrested completely above 100 K. At 300 K the slope of the curve in the slow regime seems to approach to 0.5. The curve at 260 K in the slow regime tends to become parallel to the curve at 300 K in the slow regime. This agrees well with the results reported by Roe [19,25] and the prediction from the Rouse behavior [48].

The data on the MSD are replotted in Fig. 6 as a function of temperature for several fixed values of time. At 0.1 ps, the MSD is proportional to temperature. The MSDs for 1.0, 10, and 100 ps are proportional to the temperature up to 100 K. Above 100 K they increase far rapidly with temperature. This indicates that a new molecular motion starts above about 100 K. Kanaya et al. have analyzed the MSDs in terms of temperature by QENS measurements [11]. Their results are comparable with our MSD results and they have assigned the deviation from the line proportional to the temperature to the onset of the fast process.

The self part of the intermediate scattering function (ISF) is defined as:

$$F_s(\mathbf{q}, t) = \langle \exp\{ - i\mathbf{q}[\mathbf{r}_i(t) - \mathbf{r}_i(0)]\} \rangle \quad (3)$$

where $\mathbf{r}_i(t)$ is the position vector of atom i at time t and $\mathbf{q}$ is a wave vector and the brackets $\langle\ \rangle$ represent the average for all atoms as well as for all time origins. In order to compare the obtained results with QENS results reported by Kanaya et al. [12], a $\mathbf{q}$ value of 1.65 Å^{-1} close to 1.54 Å^{-1} used in their measurement was chosen in this study. As mentioned before the incoherent neutron scattering cross section arises mainly from the hydrogen atoms. Therefore, ISFs and dynamic structure factors have to be calculated using the molecular motion of the hydrogen atoms to compare with experiments. The calculated ISFs for several temperatures are shown in

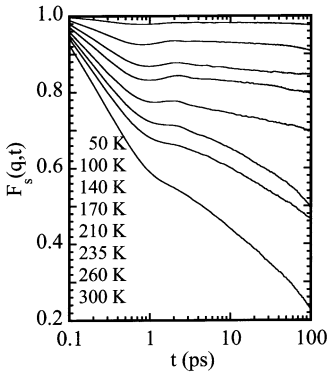

Fig. 7. The intermediate scattering functions for $\mathbf{q} = 1.65$ Å^{-1} at various temperatures.

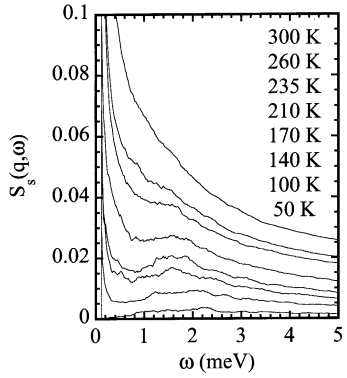

Fig. 8. The dynamic structure factors for $\mathbf{q} = 1.65$ Å^{-1} at various temperatures.

Fig. 7. The characteristics of these curves are same as the results of the MD simulations of PE [19] and PS [25] reported by Roe. Similar results have also been reported by Colmenero et al. using QENS studies of PVC [45,46]. Two regimes which corresponds to the fast and slow motions can be observed before and after the crossover of these regimes at around 1 ps. The presence of two dynamic regimes matches those seen in the MSDs in Fig. 5. Since the slope of the slow regime is almost constant at 50 K, it is expected that little conformational changes occur. At 100 K the slow regime has a negative slope indicating that the conformational changes are taking place. This implies that the α-relaxation is not completely arrested at this temperature.

The incoherent dynamic structure factor $S_s(q, \omega)$ can be evaluated by Fourier transformation of the ISF $F_s(q, t)$:

$$S_s(\mathbf{q}, \omega) = \frac{1}{2\pi} \int F_s(\mathbf{q}, t)\, e^{i\omega t}\, dt \quad (4)$$

where ω is a frequency. For the Fourier transformation, 2048 data points (204.8 ps) of the ISF were used and the Fast Fourier Transformation (FFT) method was adopted. The smoothing of $S_s(q, \omega)$ was carried out. The obtained dynamic structure factors at $\mathbf{q} = 1.65$ Å^{-1} for several temperatures are shown in Fig. 8. Below 100 K a sharp peak at 0 meV and a broad peak at around 2 meV are observed. At 235 K the broad peak at around 2 meV is degenerated into a shoulder of the sharp peak. At 300 K the broad peak at around 2 meV is no longer distinguishable from the sharp peak at 0 meV. The similar behavior has been reported by Roe using the MD calculations [19,25]. In the QENS studies of PB [12,13] a sharp peak at 0 meV, which is the elastic scattering peak, and a broad peak at around 2 meV, which is assigned to the low energy excitation peak due to the vibrational motions, have been observed. This low energy excitation peak has been observed from many amorphous polymers such as PE, PS, polycarbonate, polyisobutylene and so on [5]. Roe [25] has discussed that the origin of the broad peak is the hump between the fast and slow regimes shown in the ISFs, which is also observed in Fig. 7.

The excessive intensity due to the fast process on the order of pico seconds below 2 meV has been observed for PB using the QENS study by Kanaya et al. [12]. The excessive intensity is defined as the deviation of the low energy excitation intensity from the values expected by the Bose factor. They have shown that the excessive intensity can be observed above 120 K, which is 50 K below T_g corresponding to the Vogel–Fulcher temperature. In Fig. 8 the excessive intensities are observed below 2.0 meV above 140 K. The $\mathbf{q}$ dependence of $S_s(q, \omega)$ was also evaluated. The low energy excitation peak at 100 K and the excessive intensity at 260 K in the results of the MD simulation were observed for various values of $\mathbf{q}$ ($\mathbf{q} = 1.18$, 1.65,1.88 and 2.36 Å^{-1}). The excessive intensity was independent of the $\mathbf{q}$ value. We believe that the excessive intensity observed in this study corresponds to the fast process observed in the QENS study.

4. Conclusions

MD calculations of *cis*-1,4-polybutadiene in the bulk amorphous phase were performed to examine static as well as dynamic properties. The force field parameters are optimized to reproduce the experimental data. The calculated static properties such as glass transition temperature, density, coefficient of thermal expansion, partial radial distribution functions, and structure factor are in good agreement with experiments and literature. The molecular motion is investigated with the mean square displacements, the intermediate scattering functions, and the dynamic structure factors. An onset of a new motion above 100 K, which corresponds to the fast process, was reproduced in the temperature dependence of the mean square displacements. The observed peaks and the increase in intensity observed in the calculated dynamic structure factors, which correspond to the elastic scattering, the low energy excitation and the fast process, agree with the quasielastic neutron scattering

studies. Further detail investigation is needed to elucidate the origins of the fast process.

Acknowledgements

We thank Prof. Toshiji Kanaya (Kyoto University) for his advice and useful discussion and Dr Satoru Kuwajima (Nano Simulation Associates, Japan) for the permission to use GEMS/MD in our study.

References

[1] Leutheusser E. Phys Rev A 1984;29:2765.
[2] Götze W. Z Phys 1984;56:139.
[3] Götze W, Sjögren L. Rep Prog Phys 1992;55:241.
[4] Kanaya T, Kaji K, Ikeda S, Inoue K. Chem Phys Lett 1988;150:334.
[5] Inoue K, Kanaya T, Ikeda S, Kaji K, Shibata M, Kiyanagi Y. J Chem Phys 1991;95:5332.
[6] Kanaya T, Kaji K, Inoue K. Physica B 1992;180/181:814.
[7] Suck J-B, Rudin H, Gunterdot HJ, Beck H. Phys Rev Lett 1983;50:49.
[8] Buchenau U, Nücker N, Dianoux AJ. Phys Rev Lett 1984;53:2316.
[9] Dianoux AJ, Page N, Rosenberg HM. Phys Rev Lett 1987;58:886.
[10] Kanaya T, Kaji K, Inoue K. Macromolecules 1991;24:1826.
[11] Kanaya T, Kawaguchi T, Kaji K. Physica B 1992;182:403.
[12] Kanaya T, Kawaguchi T, Kaji K. J Chem Phys 1993;98:8262.
[13] Frick B. Progr Colloid Polym Sci 1989;80:164.
[14] Li Y, Mattice WL. Macromolecules 1992;25:4942.
[15] Kim E-G, Misra S, Mattice WL. Macromolecules 1993;26:3424.
[16] Kim E-G, Mattice WL. J Chem Phys 1994;101:6242.
[17] Haliloglu T, Bahar I, Erman B, Kim E-G, Mattice WL. J Chem Phys 1996;104:4828.
[18] Gee RH, Boyd RH. J Chem Phys 1994;101:8028.
[19] Roe RJ. J Chem Phys 1994;100:1610.
[20] Mondello M, Yang H-J, Furuya H, Roe R-J. Macromolecules 1994;27:3566.
[21] Furuya H, Mondello M, Yang H-J, Roe R-J. Macromolecules 1994;27:5674.
[22] Roe R-J, Mondello M, Furuya H, Yang H-J. Macromolecules 1995;28:2807.
[23] Takeuchi H, Roe RJ. J Chem Phys 1991;94:7446.
[24] Takeuchi H, Roe RJ. J Chem Phys 1991;94:7458.
[25] Roe RJ. J Non-Cryst Solids 1998;235–237:308.
[26] Smith GD, Paul W, Monkenbusch M, Richter D. J Chem Phys 2001;114:4285.
[27] Smith GD, Paul W, Monkenbusch M, Willner L, Richter D, Qiu XH, Ediger MD. Macromolecules 1999;32:8857.
[28] Abe Y, Flory PJ. Macromolecules 1971;4:219.
[29] Okada O. Mol Phys 1998;93:153.
[30] Okada O, Oka K, Kuwajima S, Tanabe K. Mol Sim 1999;21:325.
[31] Jorgensen WL, Maxwell DS, Tirado-Rives J. J Am Chem Soc 1996;118:11225.
[32] Jorgensen WL, Madura JD, Swenson CJ. J Am Chem Soc 1984;106:6638.
[33] van Krevelen DR, Hoftyzer PJ. Properties of polymers — their estimation and correlation with chemical structure. New York: Elsevier, 1976.
[34] Nosé S. Mol Phys 1984;52:255.
[35] Nosé S, Klein ML. Mol Phys 1983;50:1055.
[36] Hoover WG. Phys Rev A 1985;31:1695.
[37] Andersen HC. J Chem Phys 1980;72:2384.
[38] Ewald P. Ann Phys 1921;64:253.
[39] Linse P, Andersen HC. J Chem Phys 1986;85:3027.
[40] Paul DR, DiBenedetto AT. J Polym Sci 1965;C10:17.
[41] Valentine RH, Ferry JD, Homma T, Ninomiya K. J Polym Sci 1968;A2:479.
[42] Brandrup J, Immergut EH. Polymer handbook. 3rd ed. New York: Wiley/Interscience, 1989.
[43] Han J, Gee RH, Boyd RH. Macromolecules 1994;27:7781.
[44] Frick B, Richter D, Ritter CL. Europhys Lett 1989;9:557.
[45] Colmenero J. Physica A 1993;201:38.
[46] Colmenero J, Arbe A, Alegria A. J Non-Cryst Solids 1994;172/174:126.
[47] Kanaya T, Kawaguchi T, Kaji K. J Chem Phys 1996;104:3841.
[48] Rouse Jr. PE. J Chem Phys 1953;21:1272.